N O T I C E

THIS DOCUMENT HAS BEEN REPRODUCED FROM MICROFICHE. ALTHOUGH IT IS RECOGNIZED THAT CERTAIN PORTIONS ARE ILLEGIBLE, IT IS BEING RELEASED IN THE INTEREST OF MAKING AVAILABLE AS MUCH INFORMATION AS POSSIBLE

NASA Technical Memorandum 87142

Ellipsometric Surface Analysis of Wear Tracks Produced by Different Lubricants

(NASA-TM-87142) ELLIPSOMETRIC SURFACE ANALYSIS OF WEAR TRACKS PRODUCED BY DIFFERENT LUBRICANTS (NASA) 20 p
HC A02/MF A01 CSCL 11H

N86-12293

Unclas
G3/26 04808

James L. Lauer and Norbert Marxer
Rensselaer Polytechnic Institute
Troy, New York

and

William R. Jones, Jr.
Lewis Research Center
Cleveland, Ohio

Prepared for the
Tribology Conference
cosponsored by the American Society of Lubrication Engineers
and the American Society of Mechanical Engineers
Atlanta, Georgia, October 8–10, 1985

NASA

ELLIPSOMETRIC SURFACE ANALYSIS OF WEAR TRACKS PRODUCED BY DIFFERENT LUBRICANTS

James L. Lauer and Norbert Marxer
Rensselaer Polytechnic Institute
Troy, New York

and

William R. Jones, Jr.
National Aeronautics and Space Administration
Lewis Research Center
Cleveland, Ohio 44135

E-2769

SUMMARY

A scanning ellipsometer with high spatial resolution (20 μm) was used to analyze wear tracks generated on M-50 surfaces operated in several lubricant formulations. These formulations included a pure ester base stock of trimethylolpropane triheptanoate with additives of either (1) benzotriazole (BTZ), (2) dioctyldiphenylamine (DODPA), or (3) tricresylphosphate (TCP).

Results indicated that BTZ and TCP produced patchy oxide surface films consisting mainly of Fe_3O_4. DODPA produced a much more uniform oxide film. These findings may explain the tendency of lubricant formulations containing TCP to scuff more readily than those containing only antioxidants.

INTRODUCTION

The question as to what happens in lubricated wear tracks of bearings under elastohydrodynamic conditions which could lead to scuffing failure is not fully understood. An analytical procedure correlating surface structure or composition in the wear track with time-to-failure would be useful in the design of antiscuff additives for lubricants. To develop such a procedure it is necessary to understand the effect of common lubricating oils and additives on highly stressed nonconforming bearing surfaces.

In previous work (ref. 1) we showed that wear tracks on M-50 steel produced under high stress and lubricated in the presence of tricresylphosphate were more likely to scuff than surfaces lubricated with other formulations. It was found that these wear tracks were also more reactive toward topically applied hydrochloric acid solution than those produced in the presence of antioxidants only. Since iron is known to be chemically more active than iron oxide, one could deduce the presence of significant areas of bare of nearly bare metal in the wear track. Later, we were able to correlate the differences in reactivity with different oxidation patterns in the wear track (ref. 2). The oxidation of the track surface was not uniform, but proceeded at different rates on different areas.

Auger electron spectroscopy (AES) has been used as a technique for the analysis of wear track surfaces. AES requires ultrahigh vacuum and electron bombardment and is therefore not a fast, nondestructive analytical technique.

It also does not directly provide surface film thickness and composition. We therefore applied ellipsometry to this problem in the present study. We built an electronic ellipsometer of high spatial resolution (20 μm diam spot size) and high precision in determining the ellipsometric constants, which are characteristic of the surface structure and composition. Ellipsometry is nondestructive and may permit an estimate of the thickness of surface films. Because ellipsometry is noncontacting and of fast response, it is also a potential method for the determination of surface reaction kinetics.

With the high spatial resolution of our ellipsometer we were able to scan across wear tracks and determine the nature of the surfaces. Surface roughness presented some problems to the analysis, which were also known to other workers (refs. 3 and 4), but we were able to devise procedures to reduce them.

Therefore, the objective of this work was to analyze wear tracks on M-50 steel which were generated with an elastohydrodynamic contact simulator using various lubricant formulations. Analysis was accomplished using a high spatial resolution (20 μm) scanning ellipsometer and an Auger electron spectrometer. Formulations included a pure ester base stock (trimethyolpropane triheptanoate) with additives of either (1) benzotriazole, (2) dioctyldiphenylamine, or (3) tricresyl phosphate.

MATERIALS

Lubricants

In order to examine the effect of different additives separately the same base stock was used with different additives in the same concentrations as in the fully formulated lubricant package. The latter was designed to represent the MIL-L-23699 standard.

The base stock was the same pure synthesized material, trimethyolpropane triheptanoate (TMPTH), used in our earlier study (ref. 2). The lubricants were, in addition to the base stock, solutions in the base stock of (1) 0.0209 wt % of benzotriazole (BTZ), a corrosion inhibitor, (2) 1.036 wt % of dioctyldiphenylamine (DODPA), an antioxidant, and (3) 2.55 wt % of the antiwear additive tricresylphosphate (TCP).

Bearin Metal

Both components of the experimental ball/plate contact were made of the same alloy steel (M-50) and heat-treated according to the following specifications.

Preheat	816 °C
Harden	1110 °C
Quench	552 °C
Air cool	Room temperature
Temper (2 hr)	538 °C
Air cool	Room temperature
Temper (2 hr)	538 °C
Air cool	Room temperature
Three more tempers at	524 °C

The (martensitic) steel had the following composition: 0.80 percent carbon, 4.10 percent chromium, 1.00 percent vanadium, and 4.25 percent molybdenum. Its hardness after heat treatment was 62-63 (Rockwell C). The samples were 20.6 mm-diameter balls and 10 by 12 by 3 mm plates.

APPARATUS AND EXPERIMENTAL CONDITIONS

Ball/Plate Sliding Contact

In this rig an M-50 bearing ball of 20.6 mm-diameter was rotated by a horizontal shaft supported by two bearings and driven by an electric motor. The ball was loaded from above by an M-50 plate supported by linear bearings on a horizontal loading platform in such a way that the friction force developed in the contact could be determined from the strain generated in a leaf spring connecting the plate with the loading platform. For this purpose, a strain gauge was mounted on the leaf spring. The load could be varied by hanging weights on the loading platform. The lubricants were injected into the contact region from a reservoir at ambient temperature by a peristaltic pump. No attempt was made to deaerate the lubricants or to control the atmosphere of the contact region.

The maximum Hertzian pressure was 0.1 GPa in all the experiments. The ball speed was 220 rpm, corresponding to 0.2 m/s linear speed. The duration of every run was 30 min at which time the traction force had reached a near-steady value.

No attempt was made to control the contact temperature or to measure it. However, an estimate of the maximum surface temperature rise based on calculations by Ausherman et al. (ref. 5) indicated that the temperature may have exceeded 220 °C, the critical temperature for TCP/surface reaction according to Faut and Wheeler (ref. 6).

Sample Preparation

The M-50 plates used in the ball/plate sliding contact described above were thoroughly cleaned in alcohol and dried before they were subjected to ellipsometric analysis. The plates were polished with 0.3 μm diameter aluminum oxide powder, washed with alcohol, dried and soaked for 3 hr in the lubricants before they were placed in the ball/plate apparatus.

ELLIPSOMETRY

Ellipsometry is a sensitive optical method of surface analysis. It measures the change in the polarization state of a beam of light when it is reflected from a surface. There are many different kinds of ellipsometers. They allow the ratio of reflection coefficients (R_p and R_s) for the two component vibrations of the electric vector parallel and perpendicular to the plane of incidence respectively to be determined. The ratio of R_p/R_s is commonly expressed as

$$\frac{R_p}{R_s} = \tan(\psi)e^{i\Delta} \qquad (1)$$

This equation defines the real angles psi (ψ) and delta (Δ), which are very important in ellipsometry and are used throughout this paper. Tan(ψ) is the ratio of the amplitudes of the two complex reflection coefficients, R_p and R_s. Δ describes the differences of the phases of the two reflection coefficients, R_p and R_s. The measurement of ψ and Δ at one or more angles of incidence allows the nature of the surface to be determined: e.g., film thickness of surface films and their optical properties. The optical properties of a surface are described by the complex index of refraction $\hat{n}$.

$$\hat{n} = n + ik \qquad (2)$$

where n is the real refractive index and k is the real extinction coefficient. For nonabsorbing materials, the extinction coefficient is zero and $\hat{n} = n$.

Modulated Scanning Ellipsometer

A schematic of the ellipsometer is shown in figure 1. The light from a HeNe laser is polarized by a linear polarizer with the plane of polarization at an angle P (all angles are measured counter-clockwise, when looking towards the incoming beam, starting from the plane of incidence). Then it passes through a modulator, which consists of a solenoidal coil with a special Faraday glass cylinder on its axis. The magnetic field, generated by the current through the coil, causes the plane of polarization to change by an angle dP, which is proportional to the magnetic field (current) and the length of the cylinder (10 cm in our instrument). By driving the coil with an ac-current (500 Hz) of approximately 0.5 A, we obtain light whose plane of polarization is oscillating around P by approximately 1°. The linearly polarized light is then reflected from the surface and becomes elliptically polarized. Then the light passes through a second polarizer (called analyzer), some lenses, which give us the wanted spatial resolution (20 μm), and finally strikes the photodiode detector. An electrical feedback loop is used to set the analyzer angle A such, that the 500 Hz component, which is seen by the photodiode and the lock-in amplifier, is zero. Even when the 500 Hz frequency component of the light is zero, there is still light (dc and higher harmonics of 500 Hz) falling onto the detector.

This modulation technique allows for a very precise (0.01°) determination of the analyzer and polarizer angles. A detailed calculation shows, that for a null of the 500 Hz frequency at the detector, there is a relationship between the polarizer angle P, the sample properties (whose influence is given by ψ and Δ) and the analyzer angle A given by equation (3)

$$\tan 2P = \frac{2 \cos\Delta \tan\psi \tan A}{\tan^2\psi - \tan^2 A} \qquad (3)$$

By measuring A at different polarizer settings P, a curve similar to the ones in figure 2 can be obtained, and a very precise determination of ψ and Δ and the plane of incidence as well (for which $P = 0$ and $A = 0$) is

possible with a curve fitting technique. This method is good for determining ψ and Δ at one spot on the sample, but exceedingly time consuming when used for scanning. We, therefore, develop a method which gave us ψ and Δ independently. It can be seen from equation (3), which was derived with the quarter wave plate in figure 1 removed, that for P = 45°.

$$\psi = A \tag{4}$$

A plot of A versus displacement gives ψ directly as a function of position.

An independent determination of Δ is more difficult. The mathematical analysis shows that it is necessary to use the quarter wave plate and set the fast axis at 45°. An additional requirement is that $\sin(2A) \neq 0$. For a null of the 500 Hz frequency component we get

$$\Delta = \frac{\pi}{2} - 2P + k\pi k = 1, 2 \ldots \tag{5}$$

Without difficulties, Δ can be determined from P, which is measured as a function of sample position. With this method the analyzer is set such, that $\sin(2A) \neq 0$ and the signal from the lock-in amplifier is fed back to the polarizer.

RESULTS AND DISCUSSION

Auger Analysis

After running in oil with different lubricant formulations, the specimens were washed with alcohol and allowed to dry prior to their introduction into the Auger spectrometer. Auger spectra (5 keV electron beam, 20 μA beam current, 20 μm beam diameter) were taken from two spots within the wear track as a function of sputtering time. Approximately 10 Å is sputtered away per minute, the estimate being based on the time necessary to remove the contamination layer. For reference, a sample without a wear scar was also analyzed.

The peak to peak distances were converted to atom percentages using the appropriate sensitivity factors. The shape of the carbon peak(s) tell(s) us, whether the carbon is present as hydrocarbon or as carbide. The carbon in the reference and partly in one of the wear tracks generated in the presence of TCP was still present in the form of hydrocarbon after 2 min of sputtering. All other samples had hydrocarbon present only before sputtering occurred. The higher sensitivity factor for carbide was used, when the spectra show the presence of carbide.

The layer containing an appreciable amount of carbon is thin. The carbon content given is an upper limit, because carbon in the residual gas possibly contributes to the spectra. The same is true for oxygen.

Figure 3 shows the carbon content as a function of sputtering time for different samples. The line for the TCP sample could be misleading, because for this sample, the first sputtering time was 3 min, compared to 2 min for the others. There is more carbon initially, but the transition could be steeper. The exact distribution is not known. Figure 4 shows the oxygen

content as a function of sputtering time. For one spot with BTZ and DODPA formulations, the curve is very similar to the one for the reference, whereas for the two other spots the curve is quite different, even though the initial and final (6 min) percentages are similar to the ones for the reference. There is no maximum below the surface; the oxygen content just decreases. The TCP sample shows less oxygen on the top layer and more oxygen at around 60 Å (6 min). There is a small maximum, but deeper in the surface than for the reference. Because we have no data for sputtering times exceeding 6 min, we do not know how thick the film is.

The top layer also contains very small amounts of sulfur and nitrogen besides the strong peaks of carbon, oxygen, and iron. After long sputtering (6 min or more) small amounts of chromium, vanadium, and molybdenum, these elements being contained in M-50 steel, and some argon from the sputter gun show up in the spectra. No other elements were found, notably no phosphorus in the TCP sample.

The Auger analysis indicates, that there is a greater difference between spots within one sample than from one sample to another. A comparison between different samples would be required to find the elemental distribution within the whole wear track. Our analysis only tells us, that the surface is very inhomogeneous and gives us an idea about the materials present. The distribution of the material cannot be determined with good accuracy.

Ellipsometer Analysis

Figures 5 and 6 contain derived ψ and Δ across the wear track. The short traces were taken from one edge of the wear track to the other. In the longer traces the large variation of ψ and Δ indicates, where the scar begins and ends. The width of the wear track is approximately 400 μm. The roughness inside the wear track clearly contributes to the variations in ψ and Δ. But the variations are not merely due to the roughness. Inspection under the microscope shows patchiness inside the wear track and the Auger data support this. We also limited the acceptance angle of the light by geometry and stops of the apparatus to reduce the influence of roughness. We found a simple center line average for ψ and Δ over the wear track to be as good as any other method of data analysis: i.e., a line L was drawn parallel to the x-axis over the wear track such that the sum of the areas bounded by L and the trace above L was equal to the sum of the areas bounded by L and the trace below L. We then took the ordinate of L to be ψ and Δ within the wear track.

The first step in our calculations was to find an appropriate model for the M-50 steel sample. We measured ψ and Δ at three different angles of incidence. With these six measured quantities it is possible to determine six independent unknowns. We tried a model where we have one film with complex refractive index $\hat{n}(f)$ and thickness $d(f)$ on top of a substrate ($\hat{n}(s)$) and a model where we have only a substrate with complex refractive index $\hat{n}(s)$. Within experimental error, the simpler model (without a film) worked as well as the model with the film. Therefore, for our further calculations, the steel sample was represented by the experimentally determined complex refractive index.

$$\hat{n}(s) = 2.14 + 3.29i \qquad (6)$$

The next step was to analyze the M-50 steel sample, which was run in base oil containing TCP as an additive. ψ and Δ were measured across the wear track at two angles of incidence (fig. 5) and average values determined in the way described above. The determination of ψ and Δ inside the wear track yields a certain amount of variation as indicated in table I. For each value of ψ and Δ the parameters, n(f) and k(f) (real refractive index and real extinction coefficient, respectively) were determined. The uncertainity in ψ and Δ leads to undertainties in n(f) and k(f), which are expressed by the error bands in figure 7. The two bands overlap for a film thickness greater than 60 Å in figure 7(a) and smaller than 60 Å in figure 7(b). The only possible solution from these two figures is therefore a film thickness of 60 Å with corresponding complex refractive index

$$\hat{n}(s) = 2.42 + 1.72i \qquad (7)$$

The surface appears to be a mixture of the bulk material and iron oxides. The optical constants n and k determined above, lie between the values for the bulk material (M-50 steel) and the iron oxides (Fe_2O_3, Fe_3O_4) given in table II. To find out which iron oxide is present, we estimate the relative amount (mole fraction) x of the oxide according to

$$\hat{n}(\text{observed}) = (1 - x)\hat{n}(\text{substrate}) + x\hat{n}(\text{oxide}) \qquad (8)$$

From the experimentally determined $\hat{n}$, we can determine x using the optical constants of Fe_2O_3 and Fe_3O_4, respectively. The same can be done for k and the results are summarized in table III. From table III, we conclude that the surface consists only of Fe_3O_4 in approximately equal amounts and that Fe_2O_3 is not present, because its optical constants lead to values inconsistent with the experiments. The x determined from n and k are not exactly the same because we neglect the contribution of the carbon layer and because of experimental errors.

This finding is in good agreement with the Auger data where we found that the surface layer consists of approximately 50 percent iron oxide, 10 percent carbon, and 40 percent bulk material (from figs. 3 and 4).

Having shown that Fe_3O_4 was the major, if not the only oxide formed in the wear track, another set of experiments was performed to study the different additives. Before they were undertaken, the ball/plate apparatus was made more stable by different supports for the rotating ball. The spatial resolution of the ellipsometer was improved by a more sensitive light detector. Furthermore, a different set of plates was used from the one before, which came from the same heat-treated batch but was polished at a later time, in the same way, but not necessarily to exactly the same finish. The ψ's and Δ's now obtained from the A and P scans by equations (4) and (5) are shown in figure 7. These traces show more structure because of the improved resolution. This time the oxide was assumed to be Fe_3O_4 so that only the film thickness had to be determined. Figure 8 show the ψ's and Δ's versus the thickness of a surface layer consisting of various compositions of base steel and Fe_3O_4. A linear dependence of n and k on composition was assumed according to equation (8). It is clear that for oxide film thicknesses of 50 nm or less ψ is below that of the base steel and Δ above that of the base steel.

This is true for ψ's and Δ's averaged over the entire wear track for all the additives. If we look at the excursions in detail we should remember that for film thicknesses less than 30 nm, ψ decreases with film thickness while Δ increases with film thickness and for film thicknesses between 30 and 50 nm both ψ and Δ decrease with film thickness (fig. 8). For film thicknesses between about 50 and 70 nm, depending on the oxide concentrations, ψ and Δ again change in the opposite way, and for film thicknesses beyond 70 nm, they again change in the same way. Therefore the determination of film thickness from such data alone is very complex for film thicknesses exceeding 30 nm and more information is needed. The additional input could come from the use of different wavelengths or different angles in the ellipsometer.

Because ψ assumes the same values in certain regions inside the wear track as outside the wear track, one can conclude that the oxide layers inside the wear track are patchy. Minima of ψ and maxima of Δ (fig. 7) require an oxide content of 60 to 70 percent. Careful analysis of figures 7 and 8 shows that the average film thickness of the oxide layer in the wear track is 30 to 40 nm.

Summarizing, we can say that the film is about 300 to 400 Å thick. It consists of about 70 percent iron oxide and for TCP and BTZ the film is patchy. The model developed cannot explain all the features of the scans analyzed: e.g., ψ values greater than 39.5° or the variation of ψ and Δ outside the wear track. This has certainly to do with the assumption that the M-50 steel sample is represented by a single optical constant, whereas in reality the surface composition is different from the bulk. The existence of a carbon and/or oxide film of varying thickness on the surface could explain the variation of ψ and Δ outside the wear track. By representing the M-50 steel with the one film model we would be closer to reality. The derived optical constants would have to be changed slightly. But uncertainity in the measurement does not permit a detailed calculation based on this model.

CONCLUSIONS

Our work using ellipsometry and Auger electron spectroscopy has shown that tricresylphosphate and benzotriazole additives in an ester-base lubricating oil are more likely to produce patches of nearly oxide-free surfaces in wear tracks than does an antioxidant additive such as dioctyldiphenylamine. Since oxide free surfaces are more likely to weld than oxide-covered surfaces, their greater tendency to scuff can be deduced. Although our ellipsometer and our measurement techniques have given useful data, further refinements, aimed chiefly at still higher spatial resolution are desirable to achieve a better means for evaluating scuffing resistance of lubricated surfaces.

ACKNOWLEDGEMENT

This work was supported in part by Grant NAG-3-22 from NASA Lewis Research Center and partly by Grant DAAG 2483K0058 from the Army Research Office. We thank Prof. John B. Hudson for the Auger work.

REFERENCES

1. Lauer, J.L., Fung, S.S., and Jones, W.R. Jr., "Topological Reaction Rate Measurements Related to Scuffing," ASLE Trans., 27, 288-294 (1984).

2. Lauer, J.L., Marxer, N. and Jones, W.R. Jr., "Optical and Other Properties Changes of M-50 Bearing Steel Surfaces for Different Lubricants and Additives Prior to Scuffing," ASLE Prepring No. 84-LC-2A-3, (1984).

3. Smith, T., "Effect of Surface Roughness on Ellipsometry of Aluminum," Surf. Sci., 56, 252-271 (1976).

4. Vorburger, T.V., and Ludema, K.C., "Ellipsometry of Rough Surfaces," Appl. Opt., 19, 561-573 (1980).

5. Ausherman, V.K., Nagaraj, H.S., Sanborn, D.M., and Winer, W.O., "Infrared Temperature Mapping in Elastohydrodynamic Lubrication," J. Lubr. Technol., 98, 236-243 (1976).

6. Faut, O.D., and Wheeler, D.R., "On the Mechanism of Lubrication by Tricresylphosphate (TCP) - The Coefficient of Friction as a Function of Temperature for TCP on M-50 Steel," ASLE Trans., 26, 344-350 (1983)

7. Monin, J., and Boutry, G.A., "Concept Realization and Performance of a New Ellipsometer," Nouv. Rev. Opt. Appl., 4, 159-169 (1973).

8. Sullo, N.J., "Measurement of Absolute Refractive Index Profiles in Gradient Index Materials Using Modulation Ellipsometry," M.S. Thesis, University of Rochester, (1982).

9. Azzam, R.M.A., and Bashara, N.M., Ellipsometry and Polarized Light, North Holland, Amsterdam, (1977).

10. Leberknight, C.E., and Lustman, B., "An Optical Investigation of Oxide Films on Metals." J. Opt. Soc. Am., 29, 59-66 (1939).

11. Durde, P., Ann. Physik, 39, 481 (1890).

TABLE I. - EXPERIMENTALLY DETERMINED AVERAGE ψ AND Δ INSIDE THE WEAR TRACK AT TWO ANGLES OF INCIDENCE FOR M-50 STEEL SAMPLES RUN IN BASE-OIL CONTAINING TCP AS AN ADDITIVE

Angle of incidence		
α = 45.7	$\psi = 38.8 \pm 0.2$	$\Delta = 200.2 \pm 0.2$
α = 64.0	$\psi = 31.2 \pm 0.5$	$\Delta = 232 \pm 1.0$

TABLE II. - OPTICAL CONSTANTS FOR M-50 STEEL (EXPERIMENTALLY DETERMINED) AND IRON OXIDES (FROM LEBER-KNIGHT 10)

M-50 steel	$\hat{n} = 2.14 + 3.29i$
Fe_2O_3	$\hat{n} = 3.02 + 0.85i$
Fe_3O_4	$\hat{n} = 2.57 + 0.25i$

TABLE III. - CALCULATED RELATIVE AMOUNT (MOLE FRACTION) OF OXIDE (x) FROM THE EXPERIMENTALLY FOUND COMPLEX REFRACTIVE INDEX FOR THE FILM ($\hat{n}_F$ = 2.42 + 1.72i) USING EQUATION (8)

		x
Fe_2O_3	From n	0.32
	From k	0.64
Fe_3O_4	From n	0.65
	From k	0.52

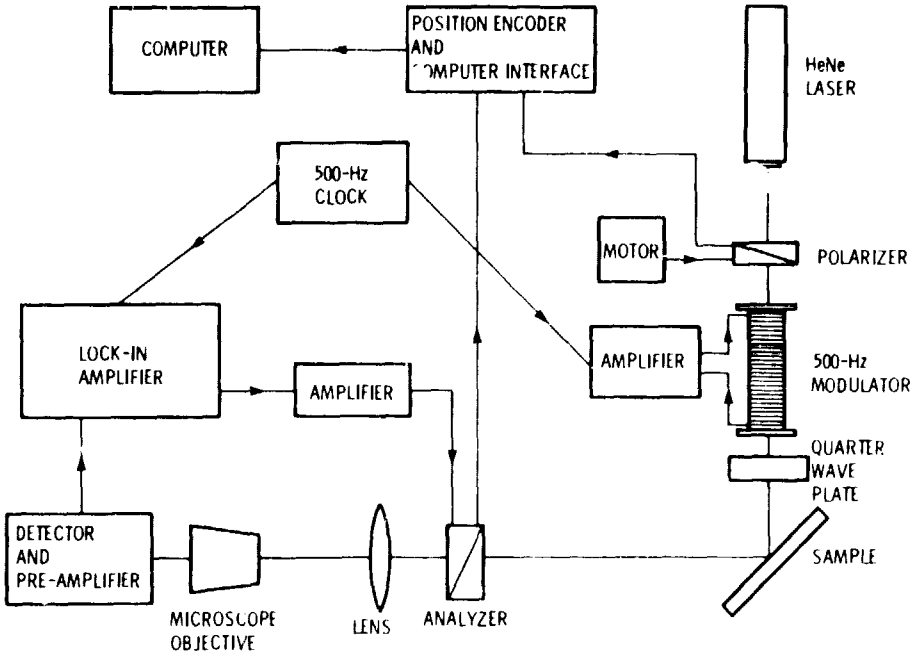

Figure 1. - Schematic of ellipsometer.

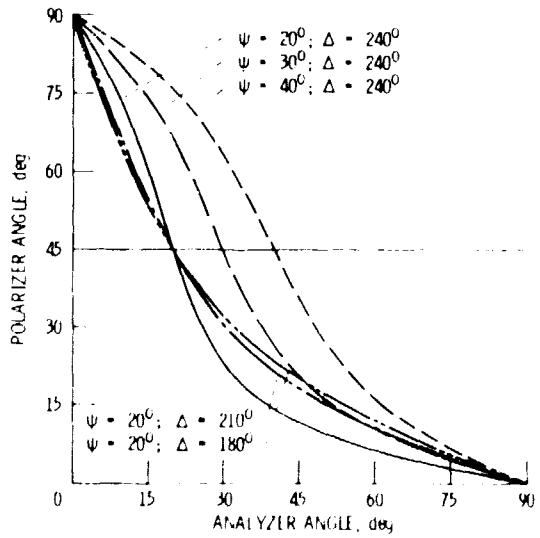

Figure 2. - Polarizer angle versus analyzer angle for different ellipsometer constants ψ and Δ.

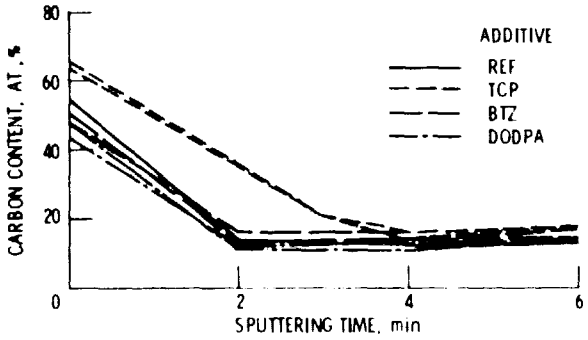

Figure 3. - Relative carbon content versus sputtering time for specimens run in base oil containing DODPA, BTZ, or TCP as an additive.

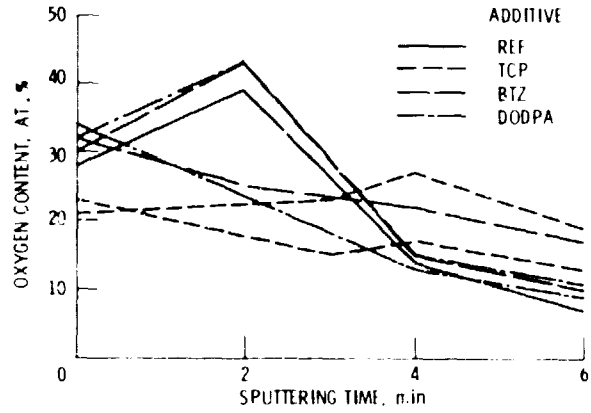

Figure 4. - Relative oxygen content versus sputtering time for specimens run in base oil containing DODPA, BTZ, OR TCP as an additive.

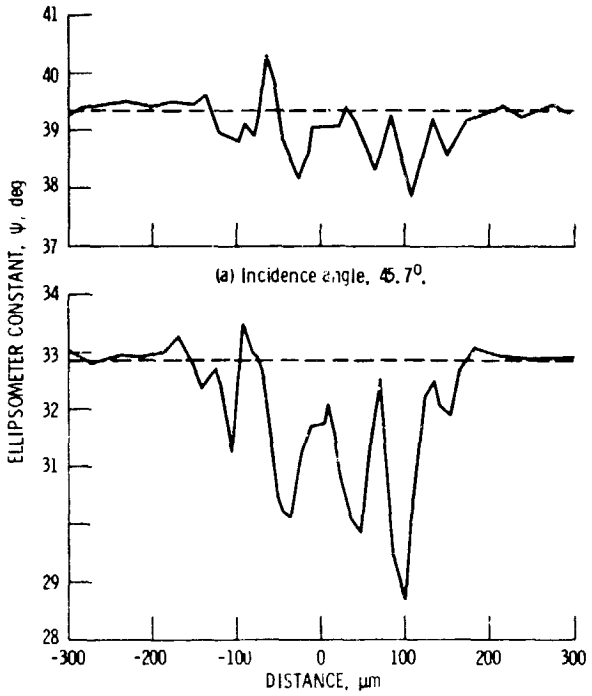

(a) Incidence angle, 45.7°.

(b) Incidence angle, 64.0°.

Figure 5. - Variation of ellipsometer constant Ψ over wear track generated with TCP. Broken line corresponds to value in absence of oxide coating.

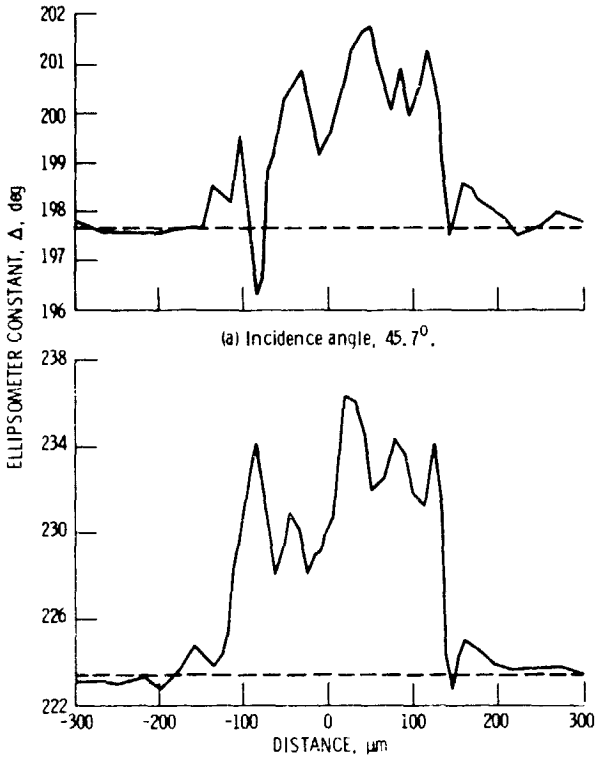

(a) Incidence angle, 45.7°.

(b) Incidence angle, 64.0°.

Figure 6. - Variation of ellipsometer constant Δ over wear track generated with TCP. Broken line corresponds to value in absence of oxide coating.

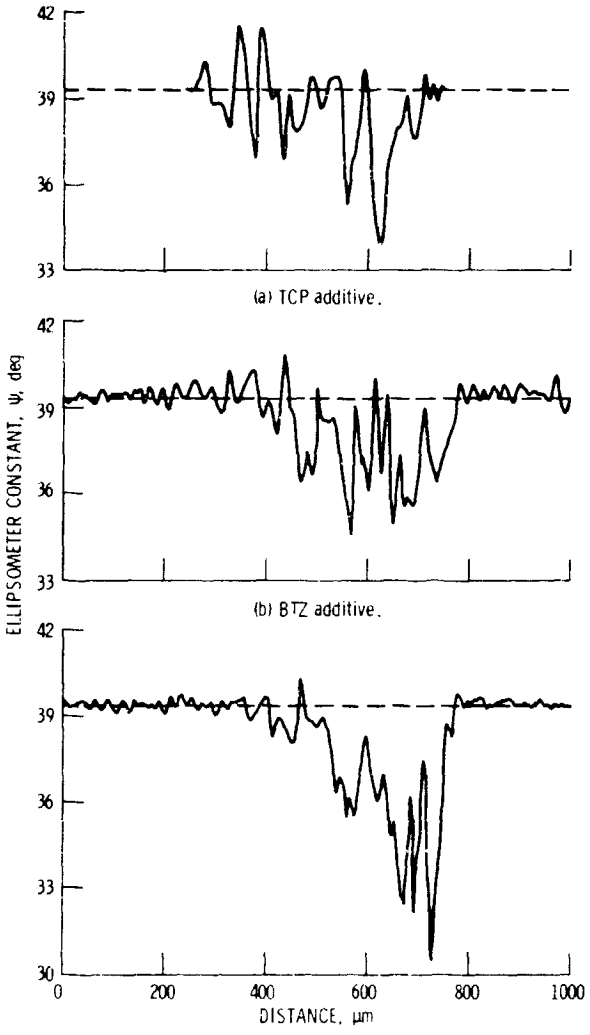

Figure 7. - Variation of ellipsometer constant ψ over wear track generated with various additives. Broken line corresponds to to value in absence of oxide coating.

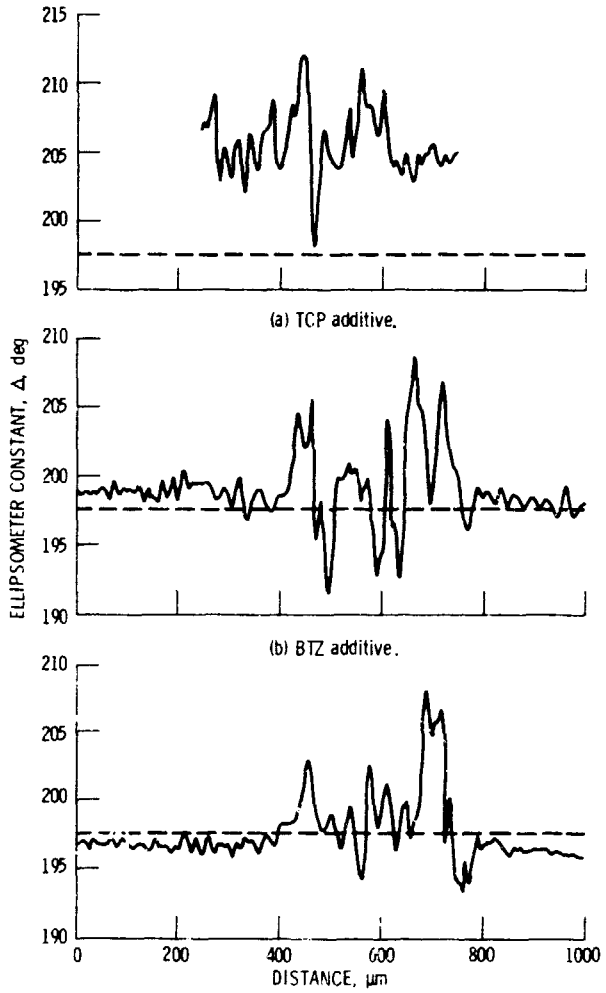

Figure 8. - Variation of ellipsometer constant Δ over a wear track generated with various additives. Broken line corresponds to value in absence of oxide coating.

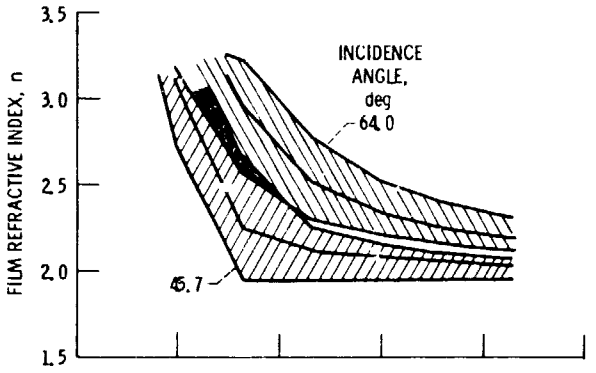

(a) Film refractive index.

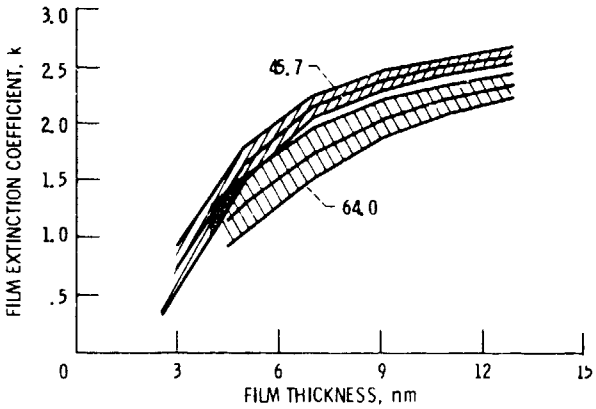

(b) Film extinction coefficient.

Figure 9. - Refractive index and extinction coefficient (with error bands) calculated from ellipsometer constants ψ and Δ given in table I for two incidence angles.

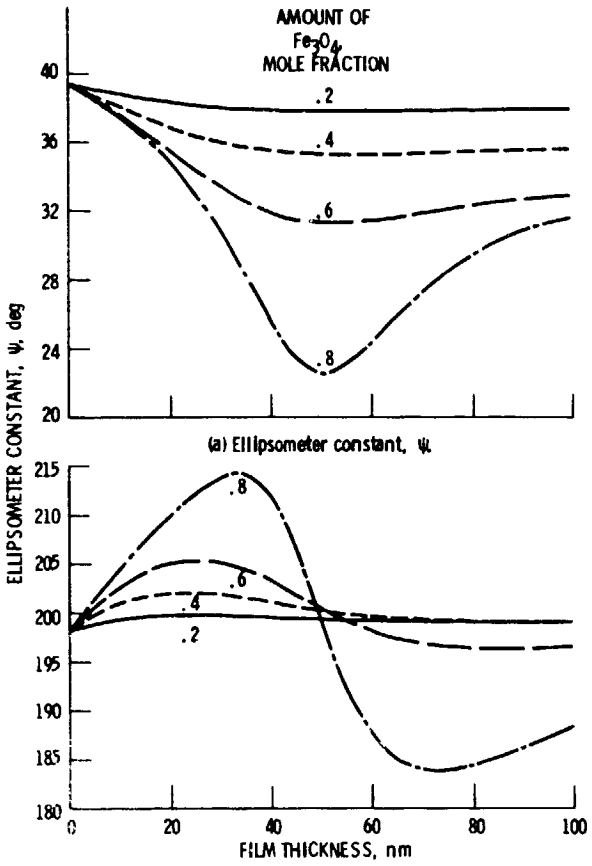

Figure 10. - Ellipsometer constants versus film thickness calculated for films containing different amounts of Fe_3O_4 on top of surface with complex refractive index $n_s = 2.14 + 3.29\,i$.

1. Report No.	2. Government Accession No.	3. Recipient's Catalog No.
NASA TM-87142		

4. Title and Subtitle	5. Report Date
Ellipsometric Surface Analysis of Wear Tracks Produced by Different Lubricants	6. Performing Organization Code: 505-33-62

7. Author(s)	8. Performing Organization Report No.
James L. Lauer, Norbert Marxer, and William R. Jones, Jr.	E-2769
	10. Work Unit No.

9. Performing Organization Name and Address	11. Contract or Grant No.
National Aeronautics and Space Administration Lewis Research Center Cleveland, Ohio 44135	13. Type of Report and Period Covered: Technical Memorandum

12. Sponsoring Agency Name and Address	14. Sponsoring Agency Code
National Aeronautics and Space Administration Washington, D.C. 20546	

15. Supplementary Notes

Prepared for the Tribology Conference cosponsored by the American Society of Lubrication Engineers and the American Society of Mechanical Engineers, Atlanta, Georgia, October 8-10, 1985. James L. Lauer and Norbert Marxer, Rensselaer Polytechnic Institute, Troy, New York. William R. Jones, Jr., NASA Lewis Research Center.

16. Abstract

A scanning ellipsometer with high spatial resolution (20 μm) was used to analyze wear tracks generated on M-50 surfaces operated in several lubricant formulations. These formulations included a pure ester base stock of trimethyol propane triheptanoate with additives of either (1) benzotriazole (BTZ), (2) dioctyldiphenylamine (DODPA), or (3) tricresylphosphate (TCP). Results indicated that BTZ and TCP produced patchy oxide surface films consisting mainly of Fe_3O_4. DODPA produced a much more uniform oxide film. These findings may explain the tendency of lubricant formulations containing TCP to scuff more readily than those containing only antioxidants.

17. Key Words (Suggested by Author(s))	18. Distribution Statement
Ellipsometry; Wear; Lubricants	Unclassified - unlimited STAR Category 26

19. Security Classif. (of this report)	20. Security Classif. (of this page)	21. No. of pages	22. Price*
Unclassified	Unclassified		

*For sale by the National Technical Information Service, Springfield Virginia 22161